J. Fluid Mech. (1996), *vol.* 313, *pp.* 367–380

Sound radiation from a cylindrical duct. Part 2. Source modelling, nil-shielding directions, and the open-to-ducted transfer function

By C. J. CHAPMAN

Department of Mathematics, University of Keele, Keele, Staffordshire, ST5 5BG, UK

(Received 27 July 1995 and in revised form 19 December 1995)

This paper analyses the sound radiated from the front face of a hard-walled circular cylindrical duct in a subsonic mean flow when the duct contains acoustic sources typical of those in a ducted-fan aeroengine. Two main results are established for modes of any given frequency and circumferential order. The first result is that in certain easily calculated directions, called here the nil-shielding directions, the sound radiated by ducted sources is the same as the sound radiated by the corresponding open sources, i.e. by unducted sources of the same distribution and strength radiating into free space. Thus in these special directions the duct has no noise-shielding effect. The second result is that, in the Kirchhoff approximation, the sound radiated by the open sources in the nil-shielding directions determines the sound radiated by the ducted sources in all directions; i.e. the sound fields radiated by open and ducted sources are related by an open-to-ducted transfer function. This function is such that the sound radiated by the ducted sources is a linear combination of certain diffraction functions, in which the coefficients are given by the sound radiated by the open sources in the nil-shielding directions. The diffraction functions do not depend on the sources and are here calculated explicitly in terms of Bessel functions. The method used in the paper is Kirchhoff's approximation; within linear theory this gives the nil-shielding directions exactly, i.e. in agreement with the Wiener–Hopf solution, and gives the main beam of the radiated field, including the major side-lobes, to good accuracy. The results are relevant to the sound radiated into the forward arc by a ducted turbofan aeroengine.

1. Introduction

The aim of this paper is to describe the sound radiated from the front face of a circular cylindrical duct when the duct contains acoustic sources of some complexity. The sources are modelled in a way that is realistic for application to studies of the noise produced by high-speed ducted turbofan aeroengines, and calculations are presented for time-dependent loading sources distributed arbitrarily over the surfaces of rotating fan blades. In order to model sources having an arbitrary time-dependence, the source distribution is decomposed into a sum of terms in accordance with the mode-interaction theory of Tyler & Sofrin (1962). All calculations include the effect of a subsonic mean flow. The final result of the calculations is a description of the radiated sound field in terms of the distribution and strength of acoustic sources on the fan blades. The calculations presented are appropriate to loading sources, but the

method applies equally to sources of any type, for example to thickness sources or to quadrupole sources.

Many aspects of this problem have been studied previously. The distinctive feature of the present work is that the far-field acoustic directivity patterns produced by ducted sources are explicitly related to the corresponding patterns which would be produced if the duct were absent. In aeroengine terminology, the far-field ducted-rotor directivities are related to the far-field open-rotor directivities. The relationship between the two may be expressed by means of an open-to-ducted transfer function, and one of the main results of the paper is an explicit expression for this transfer function. Since much is known about the sound radiated by rotors in free space, such a transfer function is of use in the harder problem of determining the sound radiated by rotors in ducts. The paper makes full use of the ray structure of duct modes described in Part 1 (Chapman 1994), and includes the effect of the mean flow on the mode ray angles.

An account of ducted sources and their radiation properties is given by Goldstein (1976, analysis leading to equation 4.47, p. 212); less detailed accounts are given by Hubbard, Lansing & Runyan (1971, §4, especially the caption to figure 19, p. 329), and by Lansing (1970, e.g. equation 12, p. 329). These authors do not consider the effect of a mean flow on the radiated field, although Goldstein determines the effect of a mean flow on the acoustic field inside the duct. Homicz & Lordi (1975) determine the effect of a mean flow on the sound radiated by a single duct mode, but do not model the acoustic sources. Only a small amount of published work models ducted sources and simultaneously accounts for the effect of a mean flow on the radiated field; some work which does both is the large-scale numerical computation of Myers & Lan (1993) and Myers (1995). A survey of the duct acoustics of aeroengines is given by Eversman (1991).

One result found below is that, for a given frequency and circumferential order, the duct has no effect on the sound radiated in certain easily determined directions; i.e. in these directions the amplitude and phase are what they would have been if the duct were absent and the source strengths were the same. These 'nil-shielding directions' are the polar mode angles of the propagating modes in the duct (Chapman 1994). The result is unexpected because the duct modes are diffracted by the end of the duct in accordance with a complicated radiation integral; one could not easily foretell that in certain directions the value of the radiation integral would be independent of the distance between the sources and the end of the duct. The result amounts to an existence theorem, and depends upon a far-field interlacing property of the radiation patterns produced by modes of different radial orders: in the mode ray direction of any one of these modes, the field radiated by each of the other modes has zero amplitude. Therefore the nil-shielding result is valid even when there are propagating modes of many radial orders, for the given frequency and circumferential order.

Another result found below is that the sound field radiated in the nil-shielding directions by an open source determines the sound field radiated in all directions by a ducted source. Hence a set of diffraction functions exists, such that the following rule determines the effect of placing a duct around a source: (i) for each radial order which gives a propagating mode, determine the corresponding nil-shielding direction, and evaluate the field radiated in this direction by the open source; (ii) multiply this field value by the corresponding diffraction function; (iii) add the results. It is a little surprising that such a rule exists, because the relationship between the open and ducted directivities would at first sight be expected to depend on the radial distribution of the acoustic source strength. The fact that the radial distribution does

not enter into the rule amounts to a structure theorem for the sound radiated by ducted sources, and is a consequence of the radial-order far-field interlacing property referred to above. The rule implies the existence of an open-to-ducted transfer function constructed from the diffraction functions. These contain Bessel functions evaluated at certain functions of direction, and are calculated explicitly below. Hence an explicit expression is obtained for the open-to-ducted transfer function.

A consequence of the structure theorem is that the effect of the duct is largely determined by the number of modes which can propagate at the given frequency and circumferential order. In an extreme case, where only one such mode can propagate, an observer in the far field of the ducted source does not 'see' the open-source directivity pattern at all, only a single diffraction function, with a coefficient equal to the open-source radiation field in the single nil-shielding direction, namely that for the single propagating mode. At the other extreme, where many modes can propagate, the far field of the ducted source is almost identical to that of the corresponding open source, and differs from it by a superposed 'wiggle'. The reason is that in this case there are many nil-shielding directions, forming a dense skeleton of lines on which the fields radiated by the open source and the ducted source are equal. Thus the two directivity patterns can differ only by a wiggle, and calculation shows that the wiggle is of low amplitude.

The paper is arranged as follows. In §2 the sound radiated by ducted loading sources is calculated by Kirchhoff's approximation, and the coefficients of the various terms are expressed as source integrals taken over the surfaces of the fan blades. Hence the nil-shielding directions are determined. In §3 the open-to-ducted transfer function is constructed; in §4 the main properties of the diffraction functions are determined; and in §5 some possibilities for future work are noted.

2. Radiation from a cylindrical duct

2.1. *Coordinates and notation*

The system to be investigated is sketched in figure 1, which shows part of the surface of a fan with B blades rotating at angular speed Ω inside a hard-walled cylindrical duct of circular cross-section and radius a. A point on the duct axis and close to the fan is taken as the origin O of a Cartesian coordinate system (x, y, z), where Ox points forwards out of the duct along its axis, Oy points horizontally to the left for an observer facing forwards, and Oz points vertically upwards. The corresponding cylindrical coordinates are (r, ϕ, x), where r is the distance from the duct axis and ϕ is the azimuthal angle around the duct axis, measured from the (O, x, y)-plane; and the corresponding spherical coordinates are (R, θ, ϕ), where R is the distance from O and θ is the polar angle, measured from the forward direction of the duct axis. The distance between O and the centre of the duct face is d, and this is used as a measure of the distance of the fan from the front of the duct.

A uniform stream of air is assumed to be flowing subsonically at speed U backwards through the duct and its exterior. Thus the coordinates just defined are wind-tunnel coordinates, in which the duct, the centre of the fan, and the observer are at rest, and the air is in motion. All the results obtained below may be converted, if required, to fly-by coordinates, in which the duct and the centre of the fan move forwards at speed U, while the observer and the air are at rest. In wind-tunnel coordinates, it is convenient to apply Doppler factors to the space variables, so that formulae can be expressed in the Prandtl–Glauert coordinates defined in §2.3.

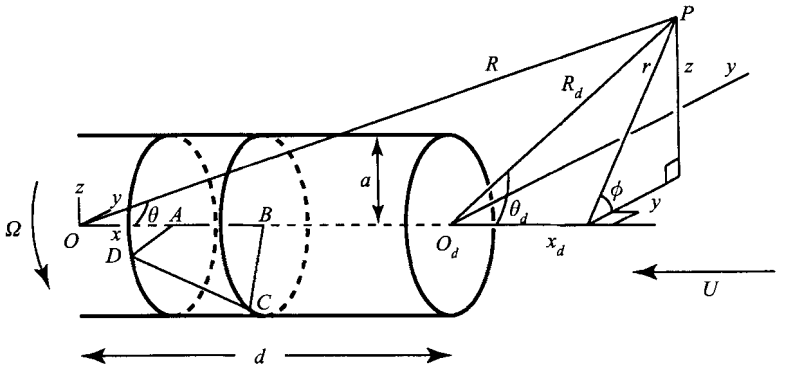

FIGURE 1. Coordinates and notation. The equation of the rotating surface $ABCD$ is $x = x^{(S)}(r, \phi - \Omega t)$. The origin O_d is at the centre of the duct face, so that the coordinates x_d, R_d, θ_d satisfy $x_d = x - d = R_d \cos\theta_d$.

Away from the sources, the acoustic pressure p satisfies the convected wave equation

$$\left\{\nabla^2 - \frac{1}{c^2}\left(\frac{\partial}{\partial t} - U\frac{\partial}{\partial x}\right)^2\right\} p = 0, \tag{2.1}$$

where t is the time and c is the speed of sound, assumed constant. Since the duct is hard-walled, the boundary condition satisfied by the pressure at $r = a$ is $\partial p/\partial r = 0$. The duct modes satisfying (2.1) are defined in §2.3.

2.2. *Source modelling*

Let us follow an infinitesimal portion of a fan blade as it rotates about the duct axis. The infinitesimal portion experiences an aerodynamic force which in general is a function of time. In accordance with the theory of Tyler & Sofrin (1962), this function of time may be decomposed into four parts:

(i) A mean part independent of time. If all B blades of the fan are considered together, the corresponding acoustic field has period $2\pi/B\Omega$ in the non-rotating frame shown in figure 1, and consists of harmonics proportional to $e^{-in(\Omega t - \phi)}$, where n is any multiple of B. This part of the acoustic field is the 'rotor-alone' or 'rotor-locked' field, i.e. the acoustic field produced by the rotation about the duct axis of a steady force exerted on the air by the fan blades.

(ii) A part with period $2\pi/\Omega$. If all B blades are considered together, the corresponding acoustic field has period $2\pi/B\Omega$ in the non-rotating frame, but the harmonics now have a more general form proportional to $e^{-i(n\Omega t - m\phi)}$, where m is any integer (the circumferential order), and n is still any multiple of B. (The special case $m = n$ reduces to case (i).) This part of the acoustic field is a 'steady distortion' field, produced by the interaction of the fan with any flow disturbance which is steady in the non-rotating frame. The disturbance could be produced by a stationary obstacle upstream of the fan, in which case the disturbance would contain an irrotational 'potential' part and a rotational 'vortical' part; or the disturbance could be produced by a stationary obstacle downstream of the fan, in which case the disturbance at the fan would contain an irrotational part only. A typical vortical part would be the viscous wake produced by a thin upstream body; the 'chopping' of the wake by the fan blades produces an acoustic field.

(iii) A part consisting of a sum of discrete Fourier components with periods other than $2\pi/\Omega$. If all B blades are considered together, the corresponding acoustic field has harmonics proportional to $e^{-i\{(n\Omega+n'\Omega')t-(n+n')\phi\}}$ in the non-rotating frame, where n is a multiple of B and n' is a multiple of a number B'. (Thus $\Omega' = 0$ gives case (ii), and $n' = 0$ gives case (i).) This part of the acoustic field is an 'unsteady distortion' field, produced by the interaction of the fan with a flow disturbance containing B' equal lobes and rotating at rate Ω'. The disturbance could be produced by a rotating obstacle upstream or downstream of the fan, for example by the potential field and by the wakes of an upstream rotor, or by the potential field of a downstream rotor. The case $\Omega = 0$ gives the acoustic field produced by the interaction of a stator with a rotating flow disturbance; the field is then of the same type as (ii), but with Ω' instead of Ω and with $n + n'$ instead of m, and the special case $n = 0$ gives a field of the same type as (i).

(iv) A part consisting of a continuum of Fourier components, i.e. a Fourier integral. If all B blades are considered together, the corresponding acoustic field has harmonics proportional to $e^{-i\{(n\Omega-\omega)t-m\phi\}}$, where n is a multiple of B and m is any integer. This broad-band field would be produced by the interaction of the fan with aperiodic flow disturbances, containing a continuum of frequencies ω. The disturbances could consist of turbulence ingested from the atmosphere or generated in the duct-wall boundary layer, or the disturbances could consist of isolated gusts and surges in the mean flow.

In what follows, all formulae are written out explicitly for case (ii), i.e. for steady distortion noise. Therefore the harmonics are taken proportional to $e^{-i(n\Omega t-m\phi)}$, where n is a multiple of B, and the final expressions for the pressure contain sums over n and m. Thus case (i) is obtained by restricting the sum to terms with $m = n$, and cases (iii) and (iv) are obtained by extending the sum to include a sum over n' or an integral over ω. These modifications may easily be obtained from the formulae below: the core of the theory emerges by examining terms proportional to $e^{-i(n\Omega t-m\phi)}$.

2.3. *Duct modes*

The duct mode of harmonic order n, circumferential order m, and radial order s is

$$e^{-in\Omega t+im\phi+ik_x x} J_m(j'_{ms} r/a), \tag{2.2}$$

where n and m are integers, and j'_{ms} is the sth zero of J'_m. Note that $j'_{01} = 0$, but that all the other j'_{ms} are non-zero.

Substitution of (2.2) into (2.1) gives the dispersion relation for duct modes. This relation is quadratic in the axial wavenumber k_x, and therefore determines two possible values of k_x for given n, m, s and Mach number $M = U/c$. The values are

$$k_x = \frac{k_n}{\beta^2}\left\{M \pm \left(1 - \left(\frac{j'_{ms}}{k_n \bar{a}}\right)^2\right)^{1/2}\right\}, \tag{2.3}$$

where $k_n = n\Omega/c$ is the free-space wavenumber corresponding to the frequency $n\Omega$, and the bar denotes division by the Doppler factor $\beta = (1 - M^2)^{1/2}$, so that $\bar{a} = a/\beta$. The analysis which follows is concerned only with propagating modes, i.e. modes for which k_x is real. It is then convenient to write k_x in terms of a mode angle $\bar{\theta}_{nms}$ lying in the range 0 to $\pi/2$ and defined by

$$\sin\bar{\theta}_{nms} = \frac{j'_{ms}}{k_n \bar{a}} = \frac{j'_{ms}}{n\bar{M}_t}, \tag{2.4}$$

where $M_t = a\Omega/c$ is the rotational Mach number, i.e. the Mach number of a hypothetical point on the duct wall rotating at angular speed Ω about the duct axis, and $\overline{M}_t = M_t/\beta$. If the radius of the duct is slightly greater than the radius of the fan, then M_t is slightly greater than the rotational tip Mach number of the fan. The most useful Doppler transformation of polar angle θ is defined by $\tan\overline{\theta} = \beta\tan\theta$; hence the angle θ_{nms} corresponding to $\overline{\theta}_{nms}$ satisfies

$$\sin\theta_{nms} = \frac{\sin\overline{\theta}_{nms}}{(1 - M^2\cos^2\overline{\theta}_{nms})^{1/2}}. \tag{2.5}$$

Note that θ_{nms} differs from the angle obtained by putting $M = 0$ in (2.4), i.e. from the angle $\theta^{(0)}_{nms}$ defined by $\sin\overline{\theta}_{nms} = \beta\sin\theta^{(0)}_{nms}$; the angle $\theta^{(0)}_{nms}$ corresponding to θ_{nms} satisfies

$$\sin\theta_{nms} = \frac{\sin\theta^{(0)}_{nms}}{(1 + M^2\sin^2\theta^{(0)}_{nms})^{1/2}}. \tag{2.6}$$

By (2.3), the propagating modes are the modes for which $j'_{ms} < k_n\bar{a}$, i.e. the modes for which $\overline{\theta}_{nms}$ is real. The upper sign in (2.3) corresponds to modes with their energy propagating forwards along the duct; the term $k_x x$ in the mode (2.2) may then be written

$$k_x x = (M + \cos\overline{\theta}_{nms})k_n\overline{\overline{x}}, \tag{2.7}$$

where $\overline{\overline{x}} = x/\beta^2$, and the mode (2.2) becomes

$$\mathrm{e}^{-\mathrm{i}n\Omega t + \mathrm{i}m\phi + \mathrm{i}(M+\cos\overline{\theta}_{nms})k_n\overline{\overline{x}}}J_m(k_n\overline{r}\sin\overline{\theta}_{nms}), \tag{2.8}$$

where $\overline{r} = r/\beta$. The mode angles $\overline{\theta}_{nms}$ determine not only the field in the duct but also the radiated field (Weinstein 1969; Rice, Heidmann & Sofrin 1979; Boyd, Kempton & Morfey 1984; Chapman 1994), i.e. the duct cannot 'hide' the ray structure of the mode from the far field. If the acoustic field is assumed to have the same frequencies in the convected and unconvected problems, as is appropriate in wind-tunnel coordinates in problems involving rotating sources, then the Doppler-transformed space variables are $\overline{\overline{x}}$ and $\overline{r}$ (see Morse & Ingard 1968, p. 722, equations 11.2.9 and 11.2.10). The Doppler-transformed polar angle $\overline{\theta}$ is then defined by $\tan\overline{\theta} = \overline{r}/\overline{\overline{x}} = \beta\tan\theta$, as was used in obtaining (2.5). The transformed variables $\overline{\overline{x}}$ and $\overline{r}$ are the Prandtl–Glauert coordinates.

2.4. *Loading integrals*

Let the surface of a fan blade inside the duct be defined by the equation $x = x^{(S)}(r, \phi - \Omega t)$, and across this surface let there be a specified pressure jump $p^{(S)}(r, \phi - \Omega t, x^{(S)}(r, \phi - \Omega t), t)$. Then acoustic modes of the form (2.8) will be excited, with coefficients proportional to certain integrals containing the pressure jump and the gradient of the complex conjugate of the mode. A full analysis is given by Goldstein (1976, pp. 195–198), from which the following details may be obtained. The required integrals are

$$T_{nm}(\overline{\theta}_{nms}) = \frac{\Omega}{2\pi}\int_0^{2\pi/\Omega}\mathrm{d}t'\int_0^{2\pi}\mathrm{d}\phi'\int_0^a e(\overline{\theta}_{nms})J_m(k_n\overline{r}'\sin\overline{\theta}_{nms})p_x r'\mathrm{d}r', \tag{2.9}$$

$$Q_{nm}(\overline{\theta}_{nms}) = \frac{\Omega}{2\pi}\int_0^{2\pi/\Omega}\mathrm{d}t'\int_0^{2\pi}\mathrm{d}\phi'\int_0^a e(\overline{\theta}_{nms})J_m(k_n\overline{r}'\sin\overline{\theta}_{nms})\frac{a}{r'}p_\phi r'\mathrm{d}r', \tag{2.10}$$

$$R_{nm}(\bar{\theta}_{nms}) = \frac{\Omega}{2\pi}\int_0^{2\pi/\Omega} \mathrm{d}t' \int_0^{2\pi} \mathrm{d}\phi' \int_0^a e(\bar{\theta}_{nms}) J'_m(k_n \bar{r}' \sin\bar{\theta}_{nms}) p_r r' \mathrm{d}r', \tag{2.11}$$

where

$$e(\bar{\theta}_{nms}) = \mathrm{e}^{\mathrm{i}(n-m)\Omega t' - \mathrm{i}m\phi' - \mathrm{i}(M+\cos\bar{\theta}_{nms})k_n \bar{\bar{x}}^{(S)}(r',\phi')} \tag{2.12}$$

and $\bar{\bar{x}}^{(S)}(r',\phi') = x^{(S)}(r',\phi')/\beta^2$. The integrals depend on the gradient, in cylindrical coordinates, of the complex conjugate of the modes (2.8); this explains the term r' in the denominator in (2.10), and the derivative of the Bessel function in (2.11). The quantities p_r, p_ϕ, p_x are evaluated at $(r', \phi', x^{(S)}(r',\phi'), t')$ and are the loading forces on the fluid per projected area in the (r',ϕ')-plane; i.e. (p_r, p_ϕ, p_x) is a vector defined so that the force on the fluid next to a surface element of area $\mathrm{d}S$ is $(p_r, p_\phi, p_x)\mathrm{d}\tilde{S}$, where $\mathrm{d}\tilde{S}$ is the projection of $\mathrm{d}S$ onto a local (r',ϕ') coordinate plane. Thus p_r, p_ϕ, p_x are determined by $p^{(S)}$ and $x^{(S)}$. Similar formulae apply if the surface of the fan blade is specified by giving r as function of $\phi - \Omega t$ and x, or by giving $\phi - \Omega t$ as a function of x and r; one of these alternatives would be used if the fan blade had a surface parallel to the duct axis, for example if the fan blade were a flat plate aligned with the flow. Expression (2.12) contains $(n-m)\Omega t'$ rather than $n\Omega t'$ because the sources are specified in rotating coordinates. The symbols T_{nm}, Q_{nm} and R_{nm} refer to thrust loading, torque loading and radial loading.

The combination of (2.9)–(2.11) which appears in the modal coefficients is

$$L_{nm}(\bar{\theta}_{nms}) = \left(\frac{M+\cos\bar{\theta}_{nms}}{\beta^2}\right) T_{nm}(\bar{\theta}_{nms}) + \frac{m}{k_n a} Q_{nm}(\bar{\theta}_{nms}) + \frac{\mathrm{i}\sin\bar{\theta}_{nms}}{\beta} R_{nm}(\bar{\theta}_{nms}), \tag{2.13}$$

and the final expression for the forward-propagating acoustic field in the duct due to the loading pressure $p^{(S)}$ on the rotating surface $x^{(S)}$ is

$$p = \sum_{nms} \frac{\mathrm{e}^{-\mathrm{i}n\Omega t + \mathrm{i}m\phi + \mathrm{i}(M+\cos\bar{\theta}_{nms})k_n \bar{\bar{x}}} J_m(k_n \bar{r} \sin\bar{\theta}_{nms})}{2\pi a^2 \gamma_{ms}^2 \cos\bar{\theta}_{nms}} L_{nm}(\bar{\theta}_{nms}), \tag{2.14}$$

where γ_{ms}^2 is a normalization factor defined by

$$\gamma_{ms}^2 = \left(1 - \frac{m^2}{j_{ms}'^2}\right) |J_m(j'_{ms})|^2 . \tag{2.15}$$

In this definition, and in all subsequent formulae, the expression $1 - m^2/j_{ms}'^2$ must be replaced by 1 when $(m,s) = (0,1)$, i.e. when $j'_{ms} = 0$. Thus $\gamma_{01}^2 = 1$. The sum is over the propagating modes and includes positive and negative n and m; but terms with $n = 0$ are excluded, because they do not correspond to an acoustic part of the pressure field. Expression (2.14) gives the acoustic field due to the loading on a single fan blade; Goldstein gives some generalizations.

2.5. *The radiation integral*

The simplest method of estimating the sound radiated from the duct face into the far field is to use Kirchhoff's approximation, in which the field at the duct face as given by (2.14) is used to determine the source strength in a free-space radiation integral. Details of the method are given in Weinstein (1969), which also contains many comparisons of Kirchhoff and Wiener–Hopf directivity patterns. Calculations of the radiation by spinning modes when there is no mean flow are given by Tyler & Sofrin (1962, Appendix C) and by Goldstein (1976, pp. 210–212). The extension to non-zero mean flow may be obtained by first applying a Lorentz transformation to

the convected wave equation (2.1) to convert it to the ordinary wave equation, and then by using Kirchhoff's approximation in the transformed coordinates. The result is that each mode (2.8) gives a radiated far field

$$\mathrm{e}^{-\mathrm{i}n\Omega t+\mathrm{i}m\phi+\mathrm{i}(M+\cos\bar{\theta}_{nms})k_n\bar{\bar{d}}}\ \mathrm{e}^{\mathrm{i}Mk_n\bar{\bar{x}}_d+\mathrm{i}k_n\bar{\bar{R}}_d}$$
$$\times(-1)(-\mathrm{i})^{m+1}\frac{\bar{a}}{\bar{\bar{R}}_d}\frac{\sin\bar{\theta}\cos\bar{\theta}_{nms}J'_m(k_n\bar{a}\sin\bar{\theta})J_m(k_n\bar{a}\sin\bar{\theta}_{nms})}{\sin^2\bar{\theta}-\sin^2\bar{\theta}_{nms}}, \tag{2.16}$$

where $\bar{\bar{x}}_d=\bar{\bar{x}}-\bar{\bar{d}}$ and $\bar{\bar{R}}_d=(\bar{\bar{x}}_d^2+\bar{r}^2)^{1/2}$. Thus x_d and R_d are coordinates measured from an origin O_d at the centre $(d,0,0)$ of the duct face (see figure 1), and $\bar{\bar{x}}_d=x_d/\beta^2$; note that the two bars on $\bar{\bar{R}}_d$ do not indicate division by β^2. In obtaining (2.16), the observation point is assumed to be in the far field, and the angles θ and θ_d shown in figure 1 have therefore been taken to be equal.

The next stage is to replace the numerator of the fraction in (2.14) by expression (2.16). The approximation $\bar{\bar{R}}_d\simeq\bar{\bar{R}}-\bar{\bar{d}}\cos\bar{\theta}$ may be used in the phase, and the approximation $\bar{\bar{R}}_d\simeq\bar{\bar{R}}$ may be used in the amplitude; the far-field radiation from the ducted source is then

$$p=\sum_{nm}\frac{(-\mathrm{i})^{m+1}k_n}{4\pi\beta^2\bar{\bar{R}}}\mathrm{e}^{-\mathrm{i}n\Omega t+\mathrm{i}m\phi+\mathrm{i}Mk_n\bar{\bar{x}}+\mathrm{i}k_n\bar{\bar{R}}}f_{nm}^{(D)}(\bar{\theta}), \tag{2.17}$$

where

$$f_{nm}^{(D)}(\bar{\theta})=\sum_s L_{nm}(\bar{\theta}_{nms})d_{nms}(\bar{\theta}) \tag{2.18}$$

and

$$d_{nms}(\bar{\theta})=\frac{-2(\sin\bar{\theta})J'_m(k_n\bar{a}\sin\bar{\theta})\mathrm{e}^{-\mathrm{i}k_n\bar{\bar{d}}(\cos\bar{\theta}-\cos\bar{\theta}_{nms})}}{k_n\bar{a}(1-m^2/j'^2_{ms})J_m(j'_{ms})(\sin^2\bar{\theta}-\sin^2\bar{\theta}_{nms})}. \tag{2.19}$$

Here the relation $j'_{ms}=k_n\bar{a}\sin\bar{\theta}_{nms}$ has been used to cancel out a term $J_m(k_n\bar{a}\sin\bar{\theta}_{nms})$ in the numerator with part of the term γ_{ms}^2 in the denominator. When $(m,s)=(0,1)$, expression (2.19) becomes

$$d_{n01}(\bar{\theta})=\frac{2J_1(k_n\bar{a}\sin\bar{\theta})\mathrm{e}^{-\mathrm{i}k_n\bar{\bar{d}}(\cos\bar{\theta}-1)}}{k_n\bar{a}\sin\bar{\theta}}, \tag{2.20}$$

on using the rule after (2.15) together with the Bessel function identity $J'_0=-J_1$ and the values $j'_{01}=0$, $\bar{\theta}_{n01}=0$. When $d=0$, this agrees with the standard formula for the sound radiated by a flat circular piston in a plane wall (Morse 1981, p. 328). The function $f_{nm}^{(D)}(\bar{\theta})$, in which the superscript D indicates 'ducted', is the polar directivity function for ducted sources. The functions $d_{nms}(\bar{\theta})$ will be called the diffraction functions.

As the distance d from the fan to the duct face is reduced, the non-propagating modes become progressively more important in determining the field at the duct face, as used in the radiation integral. The sum over s in (2.18) must then be extended to include at least some of the non-propagating modes, and in the limit $d\to 0$ they must all must be included. Then (2.18) is a sum over infinitely many s. The non-propagating modes do not present any analytical difficulty: for these modes, the polar mode angle $\bar{\theta}_{nms}$ defined by (2.4) is complex, because $j'_{ms}>k_n\bar{a}$, and so the value of k_x defined by (2.3) is also complex. Since $\sin\bar{\theta}_{nms}$ is still a real number, and $\cos\bar{\theta}_{nms}$ is now wholly imaginary, the effect on the formulae is to incorporate an exponential decay in amplitude between the fan and the duct face, but otherwise to leave the structure

of the formulae unchanged. In modern turbofan aeroengines, the large number of fan blades and the high subsonic Mach number imply that $k_n\bar{\bar{d}}$ is large unless d is very small; therefore the non-propagating modes may usually be neglected. The few modes which only just fail to propagate do not decay appreciably along the duct; but such modes affect only the sideline radiation, where Kirchhoff's approximation would not be expected to be very accurate even for the propagating modes.

Equation (2.17) is one of the main results of the paper. It is written in a form which aids comparison with the corresponding radiation pattern from open sources; this has guided the choice of source-centred coordinates (R, θ, ϕ, x) rather than face-centred coordinates $(R_d, \theta_d, \phi, x_d)$, and has also determined the notation $L_{nm}(\bar{\theta}_{nms})$ for the loading integrals.

2.6. *Radiation from open sources*

The sound radiated by a source in free space may be found by the same method as above, but with a continuum of values of the radial wavenumber; this is equivalent to taking a Hankel transform in the radial direction. Alternatively, the standard results for the sound radiated by rotating sources in a mean flow, as given by Garrick & Watkins (1954), Hanson (1983), Schulten (1988), Parry & Crighton (1989), Peake & Crighton (1991), for example, may be converted to the coordinate system and notation of the present paper. The far field requires a stationary phase calculation. The result is that the far-field radiation from an open source of the same strength and distribution as specified in §2.4 is given by an expression identical in form to (2.17), except that the polar directivity function $f^{(D)}_{nm}(\bar{\theta})$ for ducted sources is replaced by the polar directivity function $f^{(O)}_{nm}(\bar{\theta})$ for open sources, defined by

$$f^{(O)}_{nm}(\bar{\theta}) = L_{nm}(\bar{\theta}). \tag{2.21}$$

Here $L_{nm}(\bar{\theta})$ is defined by (2.13) and by the expressions which precede it, but with $\bar{\theta}_{nms}$ replaced by $\bar{\theta}$.

2.7. *Nil-shielding directions*

The numerator and denominator of expression (2.19) for $d_{nms}(\bar{\theta})$ each have a zero at the mode angle $\bar{\theta}_{nms}$, and l'Hôpital's rule shows that $d_{nms}(\bar{\theta}_{nms}) = 1$. Moreover, when $d_{nms}(\bar{\theta})$ is evaluated at the mode angle of a different radial order, i.e. at $\bar{\theta} = \bar{\theta}_{nms'}$ for $s' \neq s$, the numerator contains $J'_m(j'_{ms'})$ and so is zero, whereas the denominator is now non-zero; hence $d_{nms}(\bar{\theta}_{nms'}) = 0$ for $s' \neq s$. Thus

$$d_{nms}(\bar{\theta}_{nms'}) = \delta_{ss'}. \tag{2.22}$$

Therefore when $f^{(D)}_{nm}(\bar{\theta})$ is evaluated at a mode angle, (2.18) gives

$$f^{(D)}_{nm}(\bar{\theta}_{nms}) = L_{nm}(\bar{\theta}_{nms}). \tag{2.23}$$

But by (2.21), the right-hand side of (2.23) is the open-source directivity function evaluated at the mode angle $\bar{\theta}_{mns}$. Hence

$$f^{(D)}_{nm}(\bar{\theta}_{nms}) = f^{(O)}_{nm}(\bar{\theta}_{nms}). \tag{2.24}$$

Thus for given frequency and circumferential order, the sound radiated by a ducted source at the mode angles is identical in amplitude and phase to the sound radiated by the corresponding open source. Hence in these directions the duct has no noise-shielding effect, and the directions may be called the nil-shielding directions.

A physical argument explains the existence of nil-shielding directions. A spinning

acoustic mode propagating inside a circular cylindrical duct contains rays forming piecewise-linear helices (Chapman 1994, p. 296, figure 1*a*). The straight-line segments of these piecewise linear helices lie at the polar mode angle to the duct axis, so that, for a ducted source, an axial distance d contributes to the far field a phase term $k_n\bar{\bar{d}}\cos\bar{\theta}_{nms}$. For an open source, an axial distance d contributes to the far field a phase term $k_n\bar{\bar{d}}\cos\bar{\theta}$; this follows from figure 1 by applying a Doppler transformation to the triangle OO_dP and then resolving the line OO_d in the direction OP. Hence in the far-field direction $\bar{\theta}_{nms}$, these phase terms for the ducted and open sources are equal. On using the approximation $\bar{\bar{R}}_d \simeq \bar{\bar{R}}$ everywhere except in the phase, it then follows from the Kirchhoff radiation integrals that in the far-field direction $\bar{\theta}_{nms}$ the ducted-source radiation and open-source radiation are equal, i.e. that the direction $\bar{\theta}_{nms}$ is a nil-shielding direction. This argument suggests that the diffraction effect of the duct is produced not so much by the front part of the duct of length d, in which the field is rather similar to a field in free space, but more by the semi-infinite rear part of the duct. The physical argument illustrates the power of using mode angles to describe the duct modes – a power noted by Rice *et al.* (1979).

A consequence of the work of Weinstein (1969, pp. 104–107) is that the Kirchhoff expression (2.16) for the field radiated by the mode with parameters n, m, s agrees exactly with the Wiener–Hopf solution at the angles $\bar{\theta} = \bar{\theta}_{nms'}$ for all s'. Therefore the nil-shielding results are exact properties of the linear solution of the radiation problem. In particular, the directivity function $f^{(D)}_{nm}(\bar{\theta})$ agrees with the Wiener–Hopf directivity function at the angles $\bar{\theta} = \bar{\theta}_{nms}$ for all s, and the nil-shielding directions found here are exact on linear theory. But the source strengths are assumed to be given; therefore the effect of reflections from the duct face in modifying the source strength, possibly leading to resonance, is assumed to be already incorporated in the specification of the source distribution and strength.

The existence of nil-shielding directions is strikingly confirmed by a set of graphs in Myers & Lan (1993) obtained by numerical computation on a CRAY. For example, their figure 10 consists of superimposed polar directivity plots for different distances between a thrust-loading source and the front face of the duct. The parameter values are $n = 20, m = 20, M = 0.8, M_t = 0.9$. Therefore two radial orders give propagating modes, and (2.4)–(2.6) above give $\theta_{20,20,1} = 61°$ and $\theta_{20,20,2} = 76°$. Myers & Lan use the supplements of these angles, so that the curves in their figure 10 would be expected to cross at polar angles of 119° and 104°. Inspection of the curves reveals that they do cross at these polar angles. Figure 11 consists of the corresponding curves for a torque-loading source, and these curves, too, cross at polar angles of 119° and 104°. Figures 8 and 9 are similar, but for $M_t = 0.7$. For this value of M_t, only one radial order gives a propagating mode, and (2.4)–(2.6) give $\theta_{20,20,1} = 79°$, the supplement of which is 101°. In the figures, the curves cross at this polar angle. In figure 12, for $n = 40, m = 40, M = 0.8, M_t = 0.9$, the agreement is not quite so good: four modes propagate, and the crossings are typically about 3° away from their calculated values. This could be because at such a high frequency the radial location chosen was not far enough away from the duct face to be in the far field.

3. The open-to-ducted transfer function

Substitution of (2.21) into (2.18) gives

$$f^{(D)}_{nm}(\bar{\theta}) = \sum_s f^{(O)}_{nm}(\bar{\theta}_{nms}) d_{nms}(\bar{\theta}). \tag{3.1}$$

In this relation the acoustic sources do not enter into the diffraction functions $d_{nms}(\bar{\theta})$. Therefore the sound radiated in all directions by ducted sources is determined by the sound radiated in the nil-shielding directions $\bar{\theta}_{nms}$ by the corresponding open sources, i.e. by the terms $f_{nm}^{(O)}(\bar{\theta}_{nms})$; these terms are coefficients multiplying the 'universal' functions of angle $d_{nms}(\bar{\theta})$ given by (2.19). Relation (3.1) therefore determines an open-to-ducted transfer function. Since the functions $d_{nms}(\bar{\theta})$ are easily calculated, and only finitely many nil-shielding directions exist for given n and m, the relation is easy to use. Note that the orthogonality relation (2.22) recovers from (3.1) the result (2.24) that $f_{nm}^{(D)}(\bar{\theta}) = f_{nm}^{(O)}(\bar{\theta})$ when $\bar{\theta} = \bar{\theta}_{nms}$.

For given n and m, if only one radial order gives a propagating mode then the sum over s, i.e. over the nil-shielding directions, reduces to the single term $s = 1$. Then $f_{nm}^{(D)}(\bar{\theta})$ is proportional to $d_{nm1}(\bar{\theta})$, which is a function unrelated to open-source directivity patterns. Thus in this case the far-field of the ducted source does not 'see' the corresponding open-source directivity pattern, but only the function $d_{nm1}(\bar{\theta})$ with a coefficient determined by the open-source directivity in the single direction $\bar{\theta}_{nm1}$. But if many radial orders give propagating modes for a given n and m, then many nil-shielding directions appear in the sum (3.1), and for each of these directions the open-source and ducted-source far fields are equal. Therefore in this case the open-source directivity pattern is strongly felt, despite the presence of the duct: the difference between the two patterns is a wiggle. Thus the effect of placing a duct around a source depends largely on the number of radial orders which give propagating modes. Since the number of propagating modes increases with frequency, one conclusion is that at high frequencies a hard-walled duct does not have a profound influence on the directivity pattern of a source. This is not unexpected. For example, an analysis based on edge waves (Weinstein 1969, pp. 177–185) or on Keller cones (Chapman 1994) suggests that the rim of the end face of the duct, when irradiated by a high-frequency duct mode, acts as ring source, and that such a ring source radiates rather like an open source.

The relation (3.1) may be written

$$f_{nm}^{(D)}(\bar{\theta}) = \int_0^{\pi/2} T_{nm}(\bar{\theta}, \bar{\theta}') f_{nm}^{(O)}(\bar{\theta}') \mathrm{d}\bar{\theta}', \tag{3.2}$$

where

$$T_{nm}(\bar{\theta}, \bar{\theta}') = \sum_s d_{nms}(\bar{\theta}) \delta(\bar{\theta}' - \bar{\theta}_{nms}). \tag{3.3}$$

Thus $T_{nm}(\bar{\theta}, \bar{\theta}')$ is the open-to-ducted transfer function determined by the relation (3.1).

4. The diffraction functions

Expression (2.19) may be written

$$d_{nms}(\bar{\theta}) = \mathrm{e}^{-\mathrm{i}k_n \bar{\bar{a}}(\cos\bar{\theta} - \cos\bar{\theta}_{nms})} \tilde{d}_{ms}(j), \tag{4.1}$$

where

$$j = k_n \bar{a} \sin\bar{\theta} \tag{4.2}$$

and

$$\tilde{d}_{ms}(j) = \frac{-2jJ'_m(j)}{(1 - m^2/j'^2_{ms}) J_m(j'_{ms})(j^2 - j'^2_{ms})}. \tag{4.3}$$

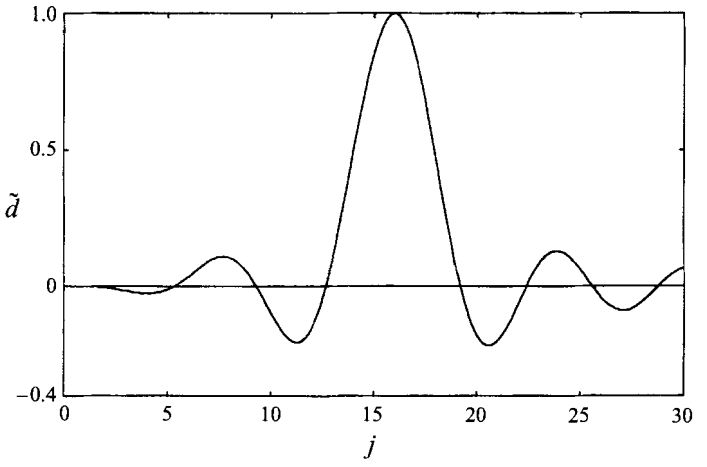

FIGURE 2. The diffraction function $\tilde{d}_{4,4}(j)$.

By (2.20), this expression becomes $\tilde{d}_{01}(j) = 2J_1(j)/j$ when $(m, s) = (0, 1)$; the small-argument limit of the Bessel function then gives $\tilde{d}_{01}(0) = 1$. The functions $d_{nms}(\bar{\theta})$ and $\tilde{d}_{ms}(j)$ differ only in phase, and for convenience they will both be called diffraction functions. Note that $\tilde{d}_{ms}(j)$ depends implicitly on n, because by (4.2) the argument j is restricted to the range $0 \leqslant j \leqslant k_n\bar{a}$; thus $j = k_n\bar{a}$ corresponds to $\bar{\theta} = \pi/2$. The orthogonality relation (2.22) for $d_{nms}(\bar{\theta})$ implies that

$$\tilde{d}_{ms}(j'_{ms'}) = \delta_{ss'}. \tag{4.4}$$

The maximum value of $\tilde{d}_{ms}$ is close to, but not exactly at, the point $j = j'_{ms}$, $\tilde{d}_{ms} = 1$.

A typical diffraction function is plotted in figure 2, which shows a graph of $\tilde{d}_{4,4}(j)$ for $0 \leqslant j \leqslant 30$. The peak is close to $j = j'_{4,4} = 15.964$, and the zeros are at $j = j'_{4,1} = 5.318, j = j'_{4,2} = 9.282, \ldots$, i.e. at $j = j'_{4,s}$ for $s \neq 4$. Recall that the relevant part of the curve depends on several parameters, including n and M, because the range $0 \leqslant \bar{\theta} \leqslant \pi/2$ corresponds to $0 \leqslant j \leqslant k_n\bar{a}$.

The diffraction functions $\tilde{d}_{4,s}(j)$ for $0 \leqslant j \leqslant 30$ are superposed in figure 3. Since $j'_{4,8} = 28.768$ and $j'_{4,9} = 31.939$, the values of s which correspond to the propagating modes are $s = 1, 2, \ldots, 8$, and the figure contains the diffraction functions for just these s. The figure makes evident the interlacing property of the curves: at the modal value $j = j'_{4,s'}$ of a curve $\tilde{d}_{4,s'}(j)$, each of the other curves has a zero; i.e. $\tilde{d}_{4,s}(j'_{4,s'}) = 0$ for $s \neq s'$. This is simply the orthogonality property (4.4). A similar set of interlacing curves, but for non-spinning modes (i.e. $m = 0$) is given in Morse (1981, p. 331, figure 71). The sum of the diffraction functions, i.e. $\sum_s \tilde{d}_{4,s}(j)$, is shown in figure 3 as a dashed curve; this curve passes through the points $(j'_{4,s}, 1)$ for $s = 1, \ldots, 8$, and may be regarded as a wiggle about a horizontal line at height 1. If the phases indicated in (4.1) are applied to $\tilde{d}_{4,s}$ before summing, the curve still passes through the points $(j'_{4,s}, 1)$, but the wiggle has a different shape. In the open-to-ducted relation (3.1), the diffraction functions are multiplied by coefficients obtained from the open-source directivity curve; the resulting ducted-source directivity curve then passes through the open-source directivity curve at the polar angles corresponding to $j'_{4,s}$, i.e. at the nil-shielding angles, and the two directivity curves interlace.

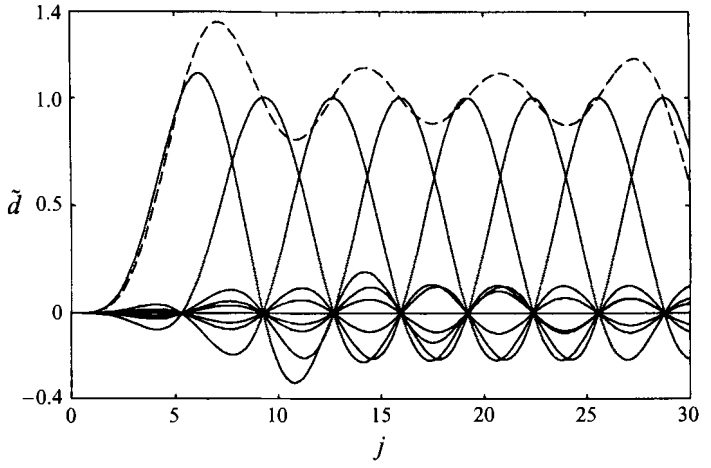

FIGURE 3. The diffraction functions $\tilde{d}_{4,s}(j)$ for $s = 1, 2, \ldots, 8$. Their sum is shown as a dashed curve.

5. Conclusion

The results above show that, in at least one problem of aeroengine acoustics, an open-to-ducted transfer function exists and can be calculated. The advantage of the transfer function approach is that a transfer function can be 'bolted-on' to existing computer codes which model the sound radiation from open rotors. It would be of interest to include in the transfer function the effects of the bell-mouth inlet, the impedance of the duct lining, and the shear in the mean flow; to obtain a realistic prediction scheme, at least some of these effects would need to be included. In modelling these effects, ray theory is likely to play a part (Lighthill 1972; Cargill 1987; Chapman 1994). Also of interest would be further theoretical analysis of the radiation pattern, using the Wiener–Hopf technique; for example, the radiation properties of duct modes may be determined exactly on linear theory, both for propagating and for non-propagating modes, and the exact linear results would make possible a calculation of the sideline and rear-arc radiation. The results of such a calculation would be particularly useful for a fan which is very close to the duct face.

Other effects will complicate the simple picture based on nil-shielding directions and on the open-to-ducted transfer function. Superposition of the sound radiated from the front and rear of an aeroengine, and from all the other noise sources on an aircraft, clearly cannot be described by a single formula; but the results of this paper provide a simple description of the sound field produced by one important source of noise.

This work has been carried out with the support of DTI (CARAD) through the Defence Research Agency, Pyestock. The author is grateful to A.B. Parry, S.J. Perkins and other members of the aeroacoustics group at Rolls-Royce, Derby, for their comments and assistance at all stages of the project.

REFERENCES

BOYD, W. K., KEMPTON, A. J. & MORFEY, C. L. 1984 Ray-theory predictions of the noise radiated from aeroengine ducts. *AIAA Paper* 84–2332.

CARGILL, A. M. 1987 A note on high frequency duct radiation. *Internal Rep., Rolls-Royce, Derby, England.*

CHAPMAN, C. J. 1994 Sound radiation from a cylindrical duct. Part 1. Ray structure of the duct modes and of the external field. *J. Fluid Mech.* **281**, 293–311.

EVERSMAN, W. 1991 Theoretical models for duct acoustic propagation and radiation. In *Aeroacoustics of Flight Vehicles: Theory and Practice. Volume 2: Noise Control* (ed. H. H. Hubbard), pp. 101–163. NASA Reference Publication 1258, vol.2.

GARRICK, I. E. & WATKINS, C. E. 1954 A theoretical study of the effect of forward speed on the free-space sound-pressure field around propellers. *NACA Rep.* 1198.

GOLDSTEIN, M. E. 1976 *Aeroacoustics*. McGraw-Hill.

HANSON, D. B. 1983 Compressible helicoidal surface theory for propeller aerodynamics and noise. *AIAA J.* **21**, 881–889.

HOMICZ, G. F. & LORDI, J. A. 1975 A note on the radiative directivity patterns of duct acoustic modes. *J. Sound Vib.* **41**, 283–290.

HUBBARD, H. H., LANSING, D. L. & RUNYAN, H. L. 1971 A review of rotating blade noise technology. *J. Sound Vib.* **19**, 227–249.

LANSING, D. L. 1970 Exact solution for radiation of sound from a semi-infinite circular duct with application to fan and compressor noise. In *Analytical Methods in Aircraft Aerodynamics*, pp. 323–334. *NASA SP*-228.

LIGHTHILL, J. 1972 The fourth annual Fairey lecture: the propagation of sound through moving fluids. *J. Sound Vib.* **24**, 471–492.

MORSE, P.M. 1981 *Vibration and Sound*. Acoustical Society of America, through the American Institute of Physics.

MORSE, P. M. & INGARD, K. U. 1968 *Theoretical Acoustics*. McGraw-Hill.

MYERS, M. K. 1995 Boundary integral formulations for ducted fan radiation calculations. *CEAS/AIAA Paper* 95–076.

MYERS, M. K. & LAN, J. H. 1993 Sound radiation from ducted rotating sources in uniform motion. *AIAA Paper* 93–4429.

PARRY, A. B. & CRIGHTON, D. G. 1989 Asymptotic theory of propeller noise – Part 1: Subsonic single-rotation propeller. *AIAA J.* **27**, 1184–1190.

PEAKE, N. & CRIGHTON, D. G. 1991 An asymptotic theory of near-field propeller acoustics. *J. Fluid Mech.* **232**, 285–301.

RICE, E. J., HEIDMANN, M. F. & SOFRIN, T. G. 1979 Modal propagation angles in a cylindrical duct with flow and their relation to sound radiation. *AIAA Paper* 79–0183.

SCHULTEN, J. B. H. M. 1988 Frequency-domain method for the computation of propeller acoustics. *AIAA J.* **26**, 1027–1035.

TYLER, J. M. & SOFRIN, T. G. 1962 Axial flow compressor noise studies. *Trans. Soc. Automotive Engrs* **70**, 309–332.

WEINSTEIN, L. A. 1969 *The Theory of Diffraction and the Factorization Method (Generalized Wiener-Hopf Technique)*. Golem.